

Contents of this file

Text S1

Figures S2 to S5

Table S6

All experiments were performed in a three-axis stressing frame constructed of flanged steel beams (Figure S2) based at the laboratories of Koninklijke/Shell Exploratie en Productie Laboratorium (KSEPL), Rijswijk, the Netherlands. A detailed description of the apparatus can be found in Browning et al., (2017). In order to provide loads perpendicular to the faces of the cubic samples along orthogonal axes, three pairs of servo-controlled hydraulic rams with a loading capacity of 300 kN and hemi-spherical seatings were used. Loading platens with an edge length of 47.5 mm were interposed between the rams and the sample faces to provide the contact surfaces. The platens are necessarily smaller than the sample faces so that a load could be applied in three-orthogonal directions simultaneously. The platens were manufactured from aluminum alloy in order to match the elastic properties of our sample material as closely as possible. By matching these properties, we reduce any edge effects, as confirmed from earlier finite element studies that simulated the distribution of stresses within cubic samples loaded in this way (e.g. Stuart, 1992; Shi et al., 2012). These studies found that, although high stress gradients occurred at the sample edges and corners, a highly uniform stress field was present throughout the bulk of the sample. To keep the sample centered within the apparatus and ensure good acoustic contact between the loading platens and the sample, a small pre-load of 4 MPa was applied along each of the three axes

prior to deformation. In-line electronic load cells with a 300 kN capacity and an accuracy of $\pm 0.2\%$ were used to measure load during deformation, and displacement in each direction was measured using LVDTs mounted between the loading platens (Browning et al., 2017) (Figure S2). Acoustic emission (AE) output was measured continuously throughout deformation using an AE transducer mounted within a recess in one of the loading platens.

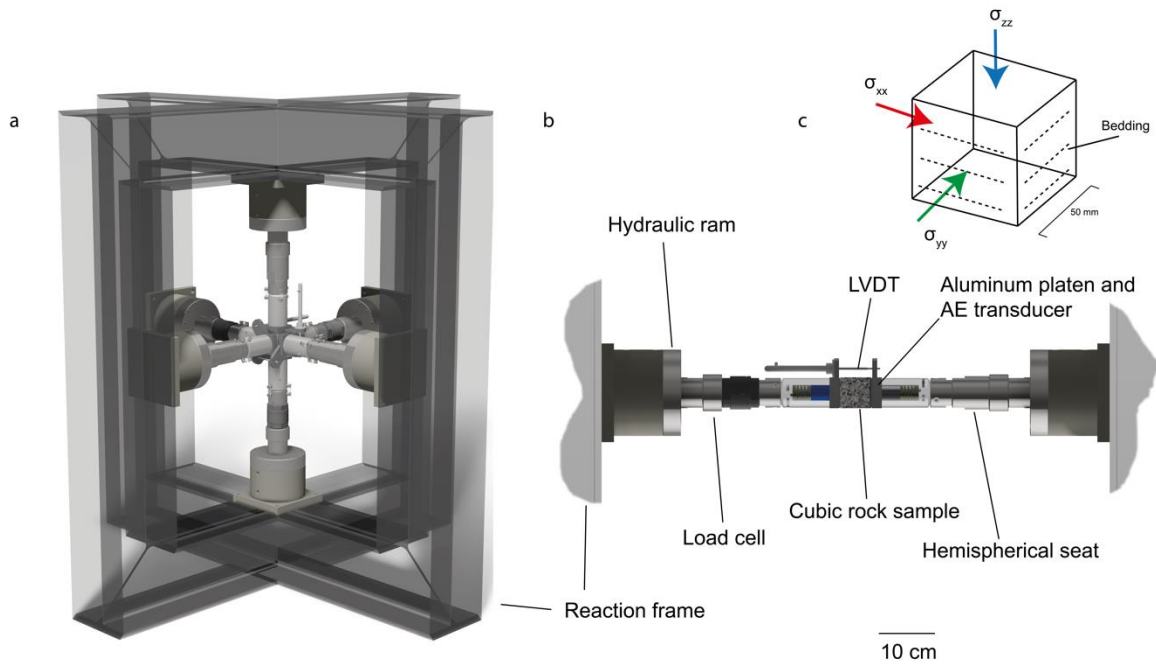


Figure S2: a) Three-axis loading frame, b) detailed schematic of loading configuration along one of the 3 loading axes, c) Loading convention used for all experiments (after Browning et al., 2017).

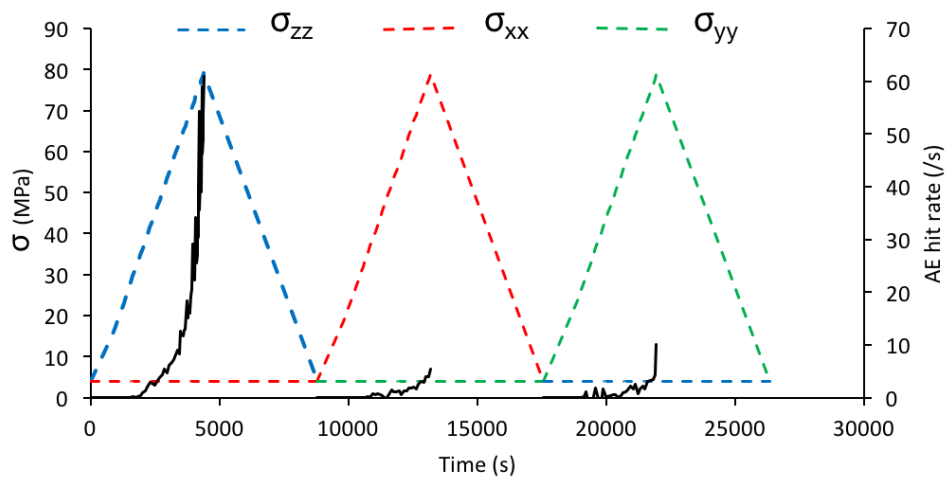


Figure S3: a) Sequential Conventional Triaxial (SCT) loading where σ_{zz} is first raised to 80 MPa and unloaded, followed in sequence by an identical loading pattern in the σ_{xx} and σ_{yy} directions. AE hits/s are denoted by a black line.

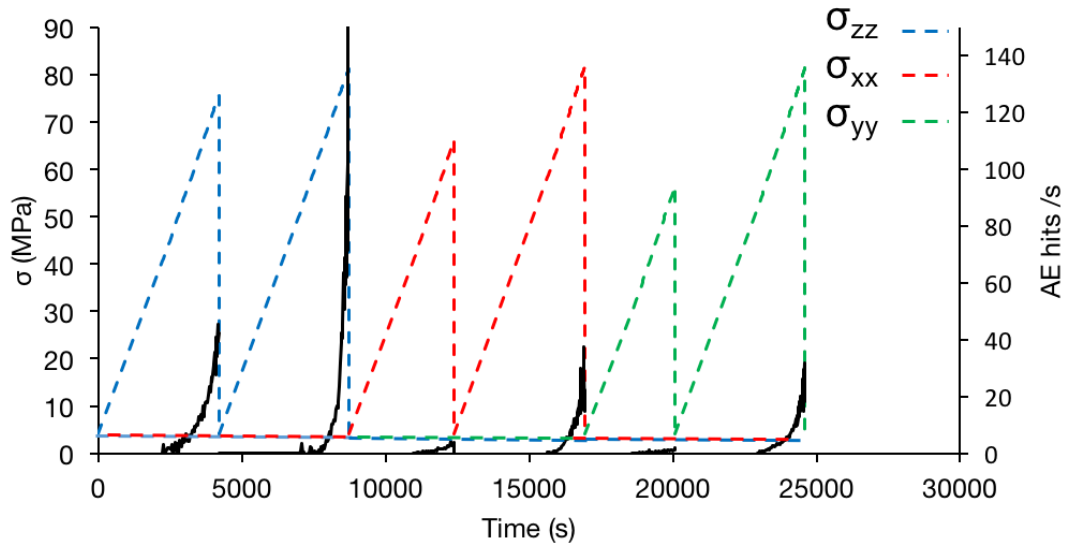


Figure S4: Cyclic Sequential Conventional Triaxial (CSCT) loading where σ_{zz} is raised to 75 MPa and then unloaded and raised higher to 80 MPa. σ_{xx} is raised to 65 MPa and 80 MPa, and σ_{yy} is raised 55 MPa and 80 MPa. AE hits/s are denoted by the black line.

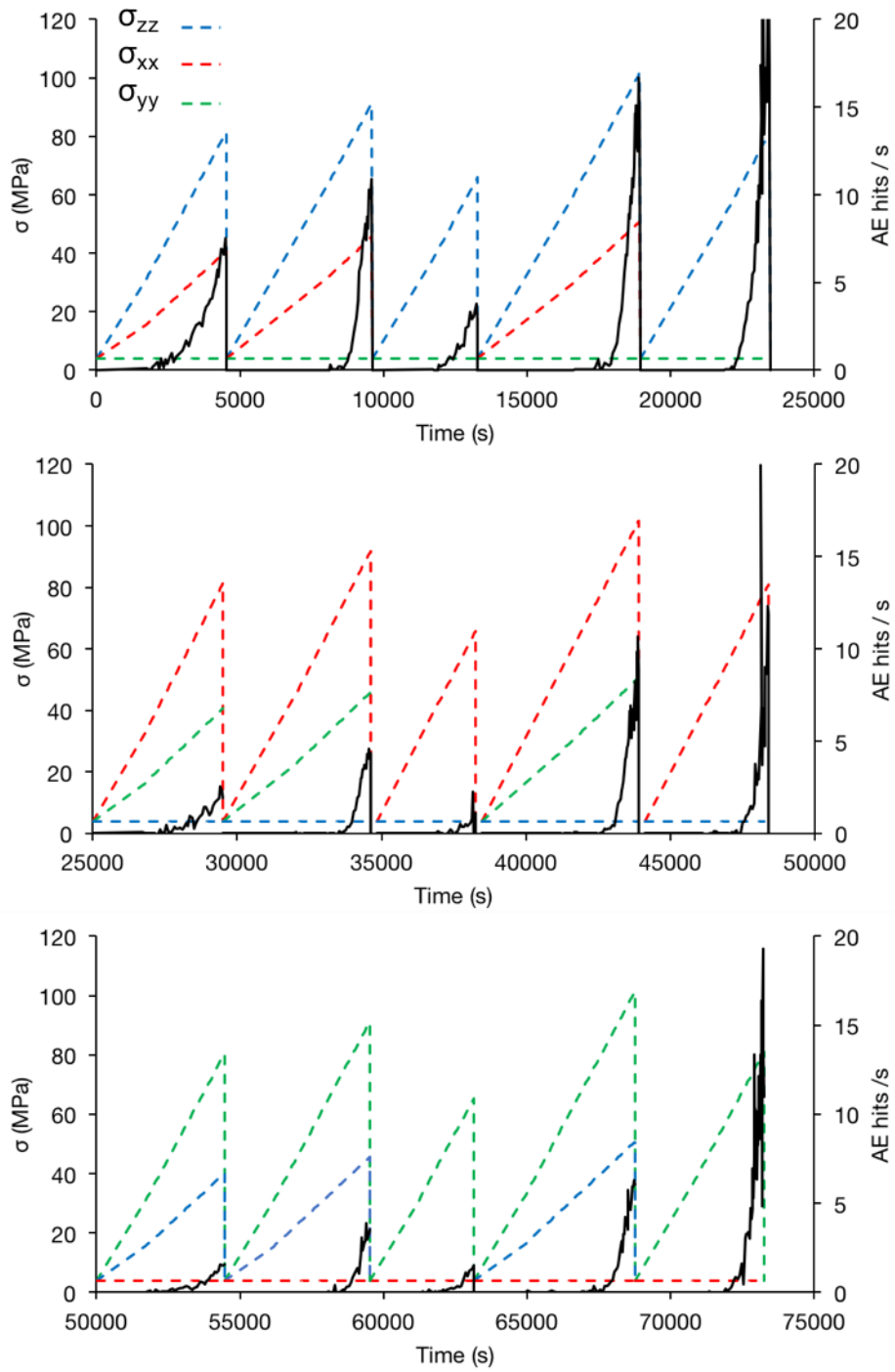


Figure S5: Cyclic Sequential True Triaxial (CSTT) loading test displaying AE hits/s.

Test number	Sample number	Test description	Stress conditions	Parameter recorded
DDSS_05	4	Sequential conventional triaxial loading to different σ_1 peaks in σ_{zz} , σ_{xx} , σ_{yy}	$\sigma_{zz} = 81$ MPa $\sigma_{xx} = \sigma_{yy} = 4$ MPa $\sigma_{xx} = 64$ MPa $\sigma_{zz} = \sigma_{yy} = 4$ MPa $\sigma_{yy} = 51$ MPa $\sigma_{xx} = \sigma_{zz} = 4$ MPa	AE σ_{zz} , σ_{xx} , σ_{yy} ε_{zz} , ε_{xx} , ε_{yy}
DDSS_06	4	Sequential conventional triaxial loading to different σ_1 peaks in σ_{zz} , σ_{xx} , σ_{yy}	$\sigma_{zz} = 72$ MPa $\sigma_{xx} = \sigma_{yy} = 4$ MPa $\sigma_{xx} = 70$ MPa $\sigma_{zz} = \sigma_{yy} = 4$ MPa $\sigma_{yy} = 57$ MPa $\sigma_{xx} = \sigma_{zz} = 4$ MPa	AE σ_{zz} , σ_{xx} , σ_{yy} ε_{zz} , ε_{xx} , ε_{yy}
DDSS_07	5	Sequential conventional triaxial loading to different σ_1 peaks in σ_{zz} , σ_{xx} , σ_{yy}	$\sigma_{zz} = 47$ MPa $\sigma_{xx} = \sigma_{yy} = 4$ MPa $\sigma_{xx} = 64$ MPa $\sigma_{zz} = \sigma_{yy} = 4$ MPa $\sigma_{yy} = 90$ MPa $\sigma_{xx} = \sigma_{zz} = 4$ MPa	AE σ_{zz} , σ_{xx} , σ_{yy} ε_{zz} , ε_{xx} , ε_{yy}
DDSS_09	6	Sequential conventional triaxial loading to different σ_1 peaks in σ_{zz} , σ_{xx} , σ_{yy}	$\sigma_{zz} = 53$ MPa $\sigma_{xx} = \sigma_{yy} = 4$ MPa $\sigma_{xx} = 64$ MPa $\sigma_{zz} = \sigma_{yy} = 4$ MPa $\sigma_{yy} = 83$ MPa $\sigma_{xx} = \sigma_{zz} = 4$ MPa	AE σ_{zz} , σ_{xx} , σ_{yy} ε_{zz} , ε_{xx} , ε_{yy}
DDSS_10	6	Sequential conventional triaxial loading to different σ_1 peaks in σ_{zz} , σ_{xx} , σ_{yy}	$\sigma_{zz} = 58$ MPa $\sigma_{xx} = \sigma_{yy} = 4$ MPa $\sigma_{xx} = 70$ MPa $\sigma_{zz} = \sigma_{yy} = 4$ MPa $\sigma_{yy} = 90$ MPa $\sigma_{xx} = \sigma_{zz} = 4$ MPa	AE σ_{zz} , σ_{xx} , σ_{yy} ε_{zz} , ε_{xx} , ε_{yy}
DDSS_17	11	Sequential conventional triaxial loading to different σ_1 peaks in σ_{zz} , σ_{xx} , σ_{yy}	$\sigma_{zz} = 80$ MPa $\sigma_{xx} = \sigma_{yy} = 4$ MPa $\sigma_{xx} = 70$ MPa $\sigma_{zz} = \sigma_{yy} = 4$ MPa $\sigma_{yy} = 60$ MPa $\sigma_{xx} = \sigma_{zz} = 4$ MPa	AE σ_{zz} , σ_{xx} , σ_{yy} ε_{zz} , ε_{xx} , ε_{yy}
DDSS_37*	29	Sequential conventional triaxial loading to different σ_1 peaks in σ_{zz} , σ_{xx} , σ_{yy}	$\sigma_{zz} = 81$ MPa $\sigma_{xx} = \sigma_{yy} = 4$ MPa $\sigma_{xx} = 81$ MPa $\sigma_{zz} = \sigma_{yy} = 4$ MPa $\sigma_{yy} = 81$ MPa $\sigma_{xx} = \sigma_{zz} = 4$ MPa	AE Wave velocities σ_{zz} , σ_{xx} , σ_{yy} ε_{zz} , ε_{xx} , ε_{yy}
DDSS_40	31	Sequential conventional triaxial loading to different	$\sigma_{zz} = 76$ MPa $\sigma_{xx} = \sigma_{yy} = 4$ MPa $\sigma_{xx} = 66$ MPa $\sigma_{zz} = \sigma_{yy} = 4$ MPa $\sigma_{yy} = 56$ MPa	AE Wave velocities σ_{zz} , σ_{xx} , σ_{yy} ε_{zz} , ε_{xx} , ε_{yy}

		σ_1 peaks in σ_{zz} , σ_{xx} , σ_{yy} Note: No AE output	$\sigma_{xx} = \sigma_{zz} = 4$ MPa	
DDSS_42	32	Sequential conventional triaxial loading to different σ_1 peaks in σ_{zz} , σ_{xx} , σ_{yy}	$\sigma_{zz} = 76$ MPa $\sigma_{xx} = \sigma_{yy} = 4$ MPa $\sigma_{xx} = 66$ MPa $\sigma_{zz} = \sigma_{yy} = 4$ MPa $\sigma_{yy} = 56$ MPa $\sigma_{xx} = \sigma_{zz} = 4$ MPa	AE Wave velocities σ_{zz} , σ_{xx} , σ_{yy} ε_{zz} , ε_{xx} , ε_{yy}
DDSS_43	32	Sequential conventional triaxial loading to different σ_1 peaks in σ_{zz} , σ_{xx} , σ_{yy}	$\sigma_{zz} = 81$ MPa $\sigma_{xx} = \sigma_{yy} = 4$ MPa $\sigma_{xx} = 81$ MPa $\sigma_{zz} = \sigma_{yy} = 4$ MPa $\sigma_{yy} = 81$ MPa $\sigma_{xx} = \sigma_{zz} = 4$ MPa	AE Wave velocities σ_{zz} , σ_{xx} , σ_{yy} ε_{zz} , ε_{xx} , ε_{yy}
DDSS_48*	18	Cyclic Sequential conventional triaxial loading to different σ_1 peaks in σ_{zz} , σ_{xx} , σ_{yy}	$\sigma_{zz} = 76$ and 81 MPa $\sigma_{xx} = \sigma_{yy} = 4$ MPa $\sigma_{xx} = 66$ and 81 MPa $\sigma_{zz} = \sigma_{yy} = 4$ MPa $\sigma_{yy} = 56$ and 81 MPa $\sigma_{xx} = \sigma_{zz} = 4$ MPa	AE Wave velocities σ_{zz} , σ_{xx} , σ_{yy} ε_{zz} , ε_{xx} , ε_{yy}
DDSS_53	37	Cyclic sequential true triaxial loading to different σ_1 peaks in σ_{zz} , σ_{xx} , σ_{yy}	$\sigma_{zz} = 80, 90, 100$ MPa $\sigma_{xx} = 40, 45, 50$ MPa $\sigma_{yy} = 4$ MPa $\sigma_{zz} = 70$ and 80 MPa $\sigma_{xx} = \sigma_{yy} = 4$ MPa $\sigma_{xx} = 80, 90, 100$ MPa $\sigma_{yy} = 40, 45, 50$ MPa $\sigma_{zz} = 4$ MPa $\sigma_{xx} = 70$ and 80 MPa $\sigma_{zz} = \sigma_{yy} = 4$ MPa $\sigma_{yy} = 80, 90, 100$ MPa $\sigma_{zz} = 40, 45, 50$ MPa $\sigma_{xx} = 4$ MPa $\sigma_{yy} = 70$ and 80 MPa $\sigma_{zz} = \sigma_{xx} = 4$ MPa	AE σ_{zz} , σ_{xx} , σ_{yy} ε_{zz} , ε_{xx} , ε_{yy}
DDSS_54*	38	Cyclic sequential true triaxial loading to different σ_1 peaks in σ_{zz} , σ_{xx} , σ_{yy}	$\sigma_{zz} = 80, 90, 100$ MPa $\sigma_{xx} = 40, 45, 50$ MPa $\sigma_{yy} = 4$ MPa $\sigma_{zz} = 70$ and 80 MPa $\sigma_{xx} = \sigma_{yy} = 4$ MPa $\sigma_{xx} = 80, 90, 100$ MPa $\sigma_{yy} = 40, 45, 50$ MPa $\sigma_{zz} = 4$ MPa $\sigma_{xx} = 70$ and 80 MPa $\sigma_{zz} = \sigma_{yy} = 4$ MPa	AE σ_{zz} , σ_{xx} , σ_{yy} ε_{zz} , ε_{xx} , ε_{yy}

			$\sigma_{yy} = 80, 90, 100 \text{ MPa}$ $\sigma_{zz} = 40, 45, 50 \text{ MPa}$ $\sigma_{xx} = 4 \text{ MPa}$ $\sigma_{yy} = 70 \text{ and } 80 \text{ MPa}$ $\sigma_{zz} = \sigma_{xx} = 4 \text{ MPa}$	
--	--	--	---	--

Table S6. Table of all experiments performed. * denotes experiments described in the paper.

